JACS
JOURNAL OF THE AMERICAN CHEMICAL SOCIETY

Communication

pubs.acs.org/JACS

Surface- vs Diffusion-Limited Mechanisms of Anion Exchange in $CsPbBr_3$ Nanocrystal Cubes Revealed through Kinetic Studies

Brent A. Koscher,[†,§,∥] Noah D. Bronstein,[†,§,∥] Jacob H. Olshansky,[†,§,∥] Yehonadav Bekenstein,[†,§,∥] and A. Paul Alivisatos*[,†,‡,§,∥]

[†]Department of Chemistry and [‡]Department of Materials Science and Engineering, University of California, Berkeley, California 94720, United States

[§]Materials Sciences Division, Lawrence Berkeley National Laboratory, Berkeley, California 94720, United States

[∥]Kavli Energy NanoScience Institute, University of California, Berkeley, and Lawrence Berkeley National Laboratory, Berkeley, California 94720, United States

Supporting Information

ABSTRACT: Ion-exchange transformations allow access to nanocrystalline materials with compositions that are inaccessible via direct synthetic routes. However, additional mechanistic insight into the processes that govern these reactions is needed. We present evidence for the presence of two distinct mechanisms of exchange during anion exchange in $CsPbX_3$ nanocrystals (NCs), ranging in size from 6.5 to 11.5 nm, for transformations from $CsPbBr_3$ to $CsPbCl_3$ or $CsPbI_3$. These NCs exhibit bright luminescence throughout the exchange, allowing their optical properties to be observed in real time, in situ. The iodine exchange presents surface-reaction-limited exchanges allowing all anionic sites within the NC to appear chemically identical, whereas the chlorine exchange presents diffusion-limited exchanges proceeding through a more complicated exchange mechanism. Our results represent the first steps toward developing a microkinetic description of the anion exchange, with implications not only for understanding the lead halide perovskites but also for nanoscale ion exchange in general.

Nanocrystals (NCs) exhibit facile and unique kinetics for a variety of solid-state chemical transformations such as galvanic replacement,[1a,b] the nanoscale Kirkendall effect,[1c,d] and ion exchange.[1e,f] A new class of materials on which novel chemical transformations can be performed are lead halide perovskites. These materials have recently received much attention for their excellent optical properties with high photoluminescence quantum yields (PLQY) and sharp emission line widths that can span the visible spectrum. Synthetic protocols for lead halide perovskite NCs have recently been reported for both organic−inorganic hybrid perovskites,[2a−c] $CH_3NH_3PbX_3$ (X = Cl, Br, I), and all-inorganic perovskites,[2d] $CsPbX_3$. The $CsPbX_3$ NCs exhibit bandgap energies that present weak quantum size effects, but are readily tunable by adjusting the halide composition such that emissions can be precisely tuned over the entire visible spectrum. The ability to finely tune band gap energy for these highly luminescent materials is potentially useful for many applications, such as displays and LEDs.[3a,b] Furthermore, it was recently reported that post-synthetic modification of $CsPbX_3$ composition via a fast facile halide exchange preserves both NC shape and size.[4a−d]

Selective ion exchanges have been observed in other nanocrystalline materials, but have predominately focused on cation exchange. Notable examples include CdSe to Ag_2Se,[1e,5f] Cd_3P_2 to InP,[5a] CdS to PbS nanorods,[5b] PbE (E = S, Se, Te) to core−shell PbE/CdE,[5c] $Cu_{2-x}S$ to $CuInS_2$,[5d] and $Cu_{3-x}P$ to InP.[5e] In these cation exchanges the anionic sublattice is maintained allowing for facile ion exchange,[1e,f,6a−c] whereas the analogous anion exchange has far fewer examples in the literature and is more commonly associated with drastic morphological changes to the NC.[1c,5g,h] If a sublattice is structurally maintained during the exchange, ion exchange affords a versatile technique to separate the control of NC composition from crystallite shape, granting an ability to synthesize previously inaccessible materials.

In contrast with previous work on cation exchange, anion exchange in $CsPbX_3$ NCs[4a−d] presents sufficiently luminescent starting, intermediate, and ending NCs to enable continuous in situ monitoring of the exchange via photoluminescence (PL) measurements. While the phenomenological process was shown to occur and potentially useful for a number of applications,[2a−d,3a,b,4a−d] kinetic studies of the exchange mechanism have not been conducted. The high luminescence at all compositions and good synthetic control with high quality NCs positions the $CsPbX_3$ material system favorably for fundamental investigations of the anion-exchange process. Monitoring the optical properties during the exchange affords us a convenient method for gaining insight into the dynamics of the exchange process. Herein, we have specifically focused on the dynamics of the transformation from $CsPbBr_3$ to both $CsPbCl_3$ and $CsPbI_3$ (Figure 1A). During the exchange to $CsPbI_3$, we observe a red-shifting bandgap with time that is well described by a single exponential. Exchanging instead to $CsPbCl_3$ results in a monotonic blue-shifting bandgap; however, the time evolution is quite complex and potentially deeply informative. There are distinct time intervals of nearly constant bandgap change, each slower than the previous, suggesting that there is a variation of the exchange barrier with degree of exchange. The exchange to $CsPbI_3$ optically presents a rapidly alloying exchange, while exchange to $CsPbCl_3$ does not.

Received: August 5, 2016
Published: September 8, 2016

DOI: 10.1021/jacs.6b08178
J. Am. Chem. Soc. 2016, 138, 12065−12068

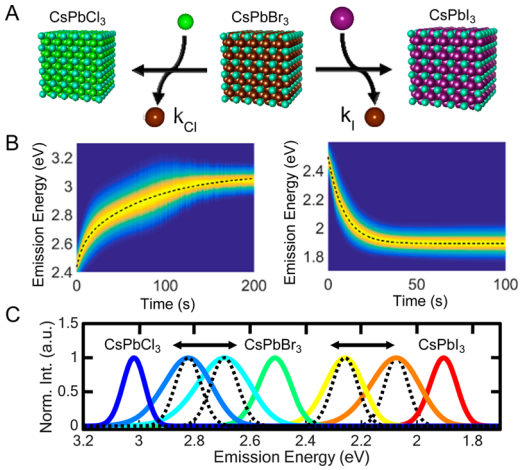

Figure 1. (A) Schematic representation of the anion-exchange reaction. (B) Representative data from the stopped-flow spectrometer showing the change in the PL spectrum over time during the exchange, $CsPbBr_3$ to $CsPbCl_3$ is on the left and $CsPbBr_3$ to $CsPbI_3$ on the right. (C) PL spectra for the starting $CsPbBr_3$ NCs (green) and ending $CsPbCl_3$ (dark blue) or $CsPbI_3$ (red) along with spectra for mixed halide compositions ($CsPbBr_{3-y}X_y$) in the both the kinetic (solid) and equilibrium (dashed) regime for each bandgap shown.

The origin of the discrepancy between the two reactions probably stems from the disparate anion sizes and ionic mobilities. Understanding the fundamental mechanisms that govern these exchanges would not only inform the development of new routes toward achieving desired products, but also generate a model system for studying the mechanism of nanoscale ion exchange.

To closely monitor the ion-exchange reactions, reagents must be mixed rapidly and reproducibly to ensure that the ensemble of NCs experiences a homogeneous environment during the exchange. This can be accomplished by using a stopped-flow injector, in which there is a submillisecond initial mixing, much faster than the many seconds required for complete ion exchange. The $CsPbBr_3$ NCs were synthesized following Protesescu et al.,[2d] with minor modifications, and present typical size dispersions of ±10% (in edge length), with PLQY typically 85−95% (Supporting Information (SI)). In our experiment, the $CsPbBr_3$ NCs and oleylammonium halide solution, both in dry hexanes, were mixed in a stopped-flow injector while real-time in situ PL spectra were obtained. The combination of submillisecond mixing time, millisecond spectral acquisition time, and good signal-to-noise (S/N > 50 at PL peak), allows for facile resolution of the exchange. A temperature controlled water bath is used to stabilize the temperature between 15 and 40 °C. A representative data set of evolving PL spectra for both exchanges is shown in Figure 1B. The observed PL spectra for homogeneous alloys (solid lines in Figure 1C), provide a direct measure of the average halide composition within the NCs, a correlation well described by Vegard's Law. When considering the kinetic intermediate mixed-halide particles, it is apparent that the ensemble PL spectra are broadened compared to the narrow line widths of the steady-state homogeneous alloys (Figure 1C). This broadening is the result of a distribution of NC sizes, which have size-dependent exchange rates. A model for this is described later in the text that accounts qualitatively for the observed broadening.

Sizes of $CsPbBr_3$ NC cubes ranging from 6.5 to 11.5 nm in edge length were studied. Monitoring the average bandgap of the distribution reveals how the average sized particle evolves with time, distinguishing the average particle from the distribution of particle sizes. The PL peak energy during exchange for a 9.0 nm sample is shown in Figure 2A,B. While the iodine exchange exhibits a single exponential trend, the chlorine exchange presents systematic deviations from exponential behavior, subtle for smaller particles than for larger ones (SI). One distinct difference in the two exchanges is seen in the changing line width throughout the exchange (Figure 2C,D), presenting consistent features irrespective of temperature. The iodine exchange displays a single prominent broadening, whereas the chlorine exchange has several distinct features, suggesting the different target anions undergo different exchange mechanisms.

Furthermore, samples from the same NC batch were monitored at a series of temperatures ranging between 15 and 40 °C. The exchange presents the same features irrespective of temperature, suggesting the exchange proceeds via the same mechanism, although the initial rate of bandgap change does increase by a factor of 5 going from 15 to 40 °C (Figure 2E), described by an Arrhenius relation. Both exchanges present a positive activation energy, 32(±1) kJ/mol for chlorine and

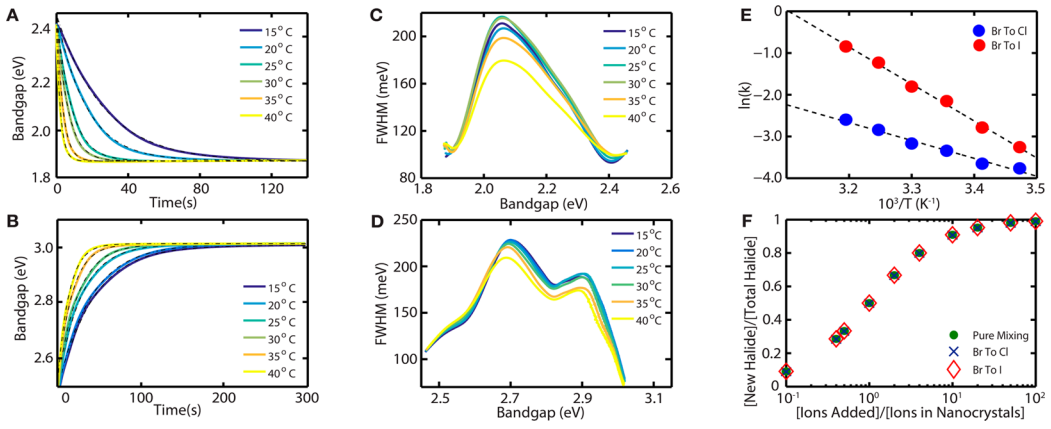

Figure 2. Temperature-dependent time progression of bandgap change for (A) $CsPbBr_3$ to $CsPbI_3$ and (B) $CsPbBr_3$ to $CsPbCl_3$, temperature ranges from 15 to 40 °C, shown for a 9.0 nm NC sample. Temperature-dependent fwhm for the (C) $CsPbBr_3$ to $CsPbI_3$ and (D) $CsPbBr_3$ to $CsPbCl_3$ exchanges. (E) Arrhenius plot fit for the temperature-dependent rate of exchange over the 15−40 °C temperature range for both exchanges. (F) Equilibrium halide composition fraction of the new halide within the NC as a function of concentration of new halide added.

DOI: 10.1021/jacs.6b08178
J. Am. Chem. Soc. 2016, 138, 12065−12068

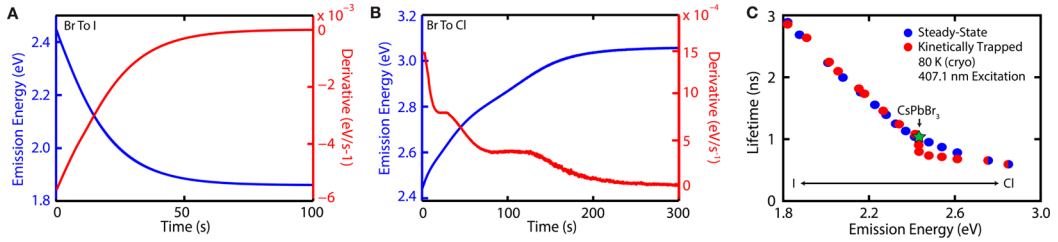

Figure 3. Time progression of bandgap change of a representative exchange reaction (blue) for (A) $CsPbBr_3$ to $CsPbI_3$ and (B) $CsPbBr_3$ to $CsPbCl_3$ with the derivative of each exchange overlaid (red). (C) Composition-dependent lifetime under pulsed 407.1 nm excitation at cryogenic temperatures (~80 K) for both steady-state alloys and kinetically trapped $CsPbX_3$ NCs. Uncertainties in the lifetimes are too small to show in the figure; all uncertainty values for the lifetimes are <1.5%.

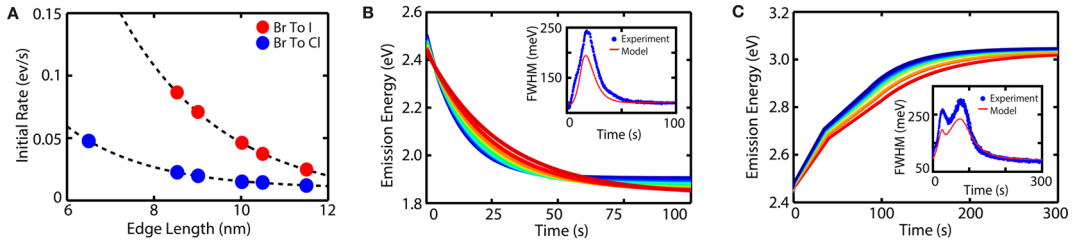

Figure 4. (A) Size-dependent initial rate of bandgap change for both exchange reactions. Model result depicting single NC exchange trajectories, where the initial bandgap is specified by color, more blue lines represent higher energy initial bandgaps, for the (B) $CsPbBr_3$ to $CsPbI_3$ and (C) $CsPbBr_3$ to $CsPbCl_3$ exchange reactions. Insets in (B) and (C) depict experimental line width change versus the exchange model.

74(±1) kJ/mol for iodine, although the interpretation of complex reaction activation energies is not straightforward without a detailed kinetic model of the many atom, multistep exchange process. However, the positive activation energy suggests the mechanism of exchange does not involve activated complexes or surface adsorption equilibria, both presenting negative apparent activation energies.[6d] We find for the material there is no thermodynamic equilibrium difference of halide ions within the material, compared to pure mixing (Figure 2F). For example, adding one halide ion for every bromine results in a 1:1 ratio in the NC, the expected ratio if there is not a thermodynamic preference for anions in the lattice. This means that any discrepancies from the equilibrium alloys are the result of kinetic processes not thermodynamic processes.

Focusing on the rate of bandgap change and the derivative of bandgap change (Figure 3A,B), we once again notice two disparate behaviors for the chlorine and iodine exchange. The iodine-exchange derivative is another exponential, whereas the chlorine-exchange derivative is something more complicated presenting discrete regions with differing constant rates of bandgap change. In fact, the chlorine exchange has regions of constant slope punctuated by sharp transitions. For the chlorine exchange there is a consistent correlation between the limits of the constant slope regions in the bandgap change and the maxima of the line width over time (SI). Particularly notable is the rate scaling of the bandgap change between the different constant rate regimes. The rate of bandgap change within a constant regime is one-half the rate of the preceding regime, independent of size (SI). We find that the exchanges undergo some consistent steps, but disparate mechanisms, for both exchanges. Independent structural determination of the distribution of the nanoparticles' anions is required to provide a definitive assignment of the origin of these different rates. However, it is notable that the rate slows in an orderly way, suggestive of systematic differences in binding energies of different sites within the NCs, such as would be expected for successive layers within a nanoparticle, or for the differences between corners, edges, and surfaces of these materials.

Due to small thermodynamic differences and low barrier to solid-state diffusion, we are unable to observe structurally the exchange using conventional structural characterization techniques. However, alloying is a solid-state diffusion process, by initiating the exchange and rapidly quenching to cryogenic temperatures (80 K) we can trap the structures by halting diffusion, and we are able to look for optical signatures of the kinetic structures. At cryogenic temperatures, the PL lifetimes for a series of kinetically trapped NCs and steady-state alloys were collected (Figure 3C). To ensure the measured PL lifetime is representative of the electron−hole overlap and not differences in nonradiative pathways, we also determined that the PLQY at 80 K is indistinguishable from unity (SI). From our study, there is no difference in the PL lifetime between kinetically trapped particles and the steady-state alloys for the iodine exchange, even though the particles are actively exchanging anions, suggesting that each particle is able to rapidly alloy. In contrast we find a noticeable deviation for the chlorine exchange, the PL lifetime for the kinetically trapped particles are not the same as the steady-state alloys, strongly suggesting the transient structures are not homogeneous alloys, but likely a more complicated, as yet undetermined, kinetic structure. During the chlorine exchange, the PL lifetime changes by 20% before the bandgap changes at all.

Although our measured rates are of bandgap change, for the iodine-exchange kinetic regime a linear Vegard's law approximation is valid, creating a direct correlation to the actual reaction rate, whereas a more complicated, nonlinear, dependence exists for the chlorine exchange. If all sites in the NC were chemically identical with a single rate-limiting step, then we would expect a monoexponential exchange. An example would be an ion exchange that is surface-limited allowing for rapid alloying, analogous to the iodine exchange. However, the presence of discrete constant bandgap change regions suggests the presence of distinct steps in the exchange. An example would be an ion exchange that is diffusion-limited resulting in the formation of

DOI: 10.1021/jacs.6b08178
J. Am. Chem. Soc. 2016, 138, 12065−12068

zones of exchange, possibly the underlying chlorine-exchange mechanism. The mechanistic discrepancy could be rationalized by considering the relative lead halide bond strengths, chlorine forms a stronger bond than iodine, resulting in slowed anion migration.[7] This exchange scheme would not be unprecedented, but analogous to the previously described extended surface reactions.[6a−c]

Finally, we investigated the kinetic regime line width changes (Figure 2C,D) to see if there is a simple explanation for their change throughout the exchange. The PL line width of an equilibrium NC ensemble is the result of the ensemble size distribution, each differently sized NC emitting at different energies. Additionally, the exchanging ensemble line width will be broader due to the size-dependent exchange rates (Figure 4A) in which small NCs, with larger bandgap, exchange faster than the larger, smaller bandgap ones for both exchanges. Additionally the chlorine exchange presents an additional consideration, namely the size-dependent transition between kinetic regimes (SI). We are able to construct a model of the exchanges by allowing a normal distribution of particle sizes, consistent with the observed size distributions, with each particle assigned its size-dependent properties including single-particle PL line widths,[8a,b] and simulate an ensemble of single-particle exchange trajectories (Figure 4B,C). With our model, we obtain a qualitative match to the observed changes in the PL line width for both exchanges (insets of Figure 4B,C). The model is able to reproduce a rather complicated exchange curve without the need for a complex model, supporting the claim that the line width change during the exchange is a convolution of the size dispersion and the underlying exchange kinetics, and not more complicated explanations such as the formation of defective particles during the exchange.

In conclusion, we have shown that, due to the excellent optical properties of $CsPbX_3$ material throughout the exchange, the anion exchange can be monitored in situ by optical methods. By carefully monitoring the optical properties during the exchange, we gain insights into the mechanism of anion exchange. Our results show that the underlying mechanism is different for the iodine and chlorine exchange. In the iodine exchange, NCs rapidly alloy and the reaction is likely surface-limited, whereas the chlorine exchange is likely diffusion-limited, producing zones of exchange. These materials show no thermodynamic preference for the different anions, so we are observing a kinetic process; as a result, at cryogenic temperatures (80 K), we are able to trap the transient structures by halting solid-state diffusion. The unique nature of the anion exchange in $CsPbX_3$ NCs places the material in a favorable position for mechanistic studies, both for understanding the lead halide perovskite materials and as a model system for fundamentally probing the general mechanism of nanoscale ion exchange.

■ ASSOCIATED CONTENT

Supporting Information

The Supporting Information is available free of charge on the ACS Publications website at DOI: 10.1021/jacs.6b08178.

Experimental details, particle characterization, and detailed descriptions of fittings (PDF)

■ AUTHOR INFORMATION

Corresponding Author

*alivis@berkeley.edu

Notes

The authors declare no competing financial interest.

■ ACKNOWLEDGMENTS

Supported by the Physical Chemistry of Inorganic Nanostructures Program (KC3103), Office of Science, Office of Basic Energy Sciences, U.S. Department of Energy (DOE), under contract DE-AC02-05CH11231

■ REFERENCES

(1) (a) Sun, Y.; Xia, Y. *Nano Lett.* **2003**, *3*, 1569. (b) Zhang, H.; Jin, M.; Wang, J.; Li, W.; Camargo, P. H. C.; Kim, M. J.; Yang, D.; Xie, Z.; Xia, Y. *J. Am. Chem. Soc.* **2011**, *133*, 6078. (c) Yin, Y.; Rioux, R. M.; Erdonmez, C. K.; Hughes, S.; Somorjai, G. A.; Alivisatos, A. P. *Science* **2004**, *304*, 711. (d) Wang, W.; Dahl, M.; Yin, Y. *Chem. Mater.* **2013**, *25*, 1179. (e) Son, D. H.; Hughes, S. M.; Yin, Y.; Alivisatos, A. P. *Science* **2004**, *306*, 1009. (f) Rivest, J. B.; Jain, P. K. *Chem. Soc. Rev.* **2013**, *42*, 89.

(2) (a) Zhang, F.; Zhong, H.; Chen, C.; Wu, X.; Hu, X.; Huang, H.; Han, J.; Zou, B.; Dong, Y. *ACS Nano* **2015**, *9*, 4533. (b) Huang, H.; Susha, A. S.; Kershaw, S. V.; Hung, T. F.; Rogach, A. L. *Adv. Sci.* **2015**, *2*, 1500194. (c) Vybornyi, O.; Yakunin, S.; Kovalenko, M. V. *Nanoscale* **2016**, *8*, 6278. (d) Protesescu, L.; Yakunin, S.; Bodnarchuk, M. I.; Krieg, F.; Caputo, R.; Hendon, C.; Yang, R. X.; Walsh, A.; Kovalenko, M. V. *Nano Lett.* **2015**, *15*, 3692.

(3) (a) Song, J.; Li, J.; Li, X.; Xu, L.; Dong, Y.; Zeng, H. *Adv. Mater.* **2015**, *27*, 7162. (b) Swarnkar, A.; Chulliyil, R.; Ravi, V. K.; Irfanullah, M.; Chowdhury, A.; Nag, A. *Angew. Chem., Int. Ed.* **2015**, *54*, 15424.

(4) (a) Akkerman, Q. A.; D'Innocenzo, V.; Accornero, S.; Scarpellini, A.; Petrozza, A.; Prato, M.; Manna, L. *J. Am. Chem. Soc.* **2015**, *137*, 10276. (b) Nedelcu, G.; Protesescu, L.; Yakunin, S.; Bodnarchuk, M. I.; Grotevent, M. J.; Kovalenko, M. V. *Nano Lett.* **2015**, *15*, 5635. (c) Ramasamy, P.; Lim, D.; Kim, B.; Lee, S.; Lee, M.; Lee, J. *Chem. Commun.* **2016**, *52*, 2067. (d) Bekenstein, Y.; Koscher, B. A.; Eaton, S. W.; Yang, P.; Alivisatos, A. P. *J. Am. Chem. Soc.* **2015**, *137*, 16008.

(5) (a) Beberwyck, B. J.; Alivisatos, A. P. *J. Am. Chem. Soc.* **2012**, *134*, 19977. (b) Luther, J. M.; Zheng, H.; Sadtler, B.; Alivisatos, A. P. *J. Am. Chem. Soc.* **2009**, *131*, 16851. (c) Pietryga, J. M.; Werder, D. J.; Williams, D. J.; Casson, J. L.; Schaller, R. D.; Klimov, V. I.; Hollingsworth, J. A. *J. Am. Chem. Soc.* **2008**, *130*, 4879. (d) van der Stam, W.; Berends, A. C.; Rabouw, F. T.; Willhammar, T.; Ke, X.; Meeldijk, J. D.; Bals, S.; de Mello Donega, C. *Chem. Mater.* **2015**, *27*, 621. (e) De Trizio, L.; Gaspari, R.; Bertoni, G.; Kriegel, I.; Moretti, L.; Scotognella, F.; Maserati, L.; Zhang, Y.; Messina, G. C.; Prato, M.; Marras, S.; Cavalli, A.; Manna, L. *Chem. Mater.* **2015**, *27*, 1120. (f) Routzahn, A. L.; Jain, P. K. *Nano Lett.* **2014**, *14*, 987. (g) Sun, H.; Chen, Y.; Wang, X.; Xie, Y.; Li, W.; Zhang, X. *J. Nanopart. Res.* **2011**, *13*, 97. (h) Park, J.; Zheng, H.; Jun, Y.; Alivisatos, A. P. *J. Am. Chem. Soc.* **2009**, *131*, 13943.

(6) (a) Baumann, S. F.; Brindley, P. K.; Smith, S. D. *Metall. Trans. A* **1990**, *21*, 1559. (b) Rai, A.; Park, K.; Zhou, L.; Zachariah, M. R. *Combust. Theory Modell.* **2006**, *10*, 843. (c) Helfferich, F. *J. Phys. Chem.* **1965**, *69*, 1178. (d) Helfferich, F. G. In *Kinetics of Multistep Reactions*, 2nd ed.; Green, N. J. B., Ed.; Comprehensive Chemical Kinetics *40*; Elsevier: Amsterdam, 2004.

(7) Dastidar, S.; Egger, D. A.; Tan, L. Z.; Cromer, S. B.; Dillon, A. D.; Liu, S.; Kronik, L.; Rappe, A. M.; Fafarman, A. T. *Nano Lett.* **2016**, *16*, 3563.

(8) (a) Hu, F.; Zhang, H.; Sun, C.; Yin, C.; Lv, B.; Zhang, C.; Yu, W. W.; Wang, X.; Zhang, Y.; Xiao, M. *ACS Nano* **2015**, *9*, 12410. (b) Park, Y.; Guo, S.; Makarov, N. S.; Klimov, V. I. *ACS Nano* **2015**, *9*, 10386.

DOI: 10.1021/jacs.6b08178
J. Am. Chem. Soc. 2016, 138, 12065−12068